Algal Research 84 (2024) 103744

Contents lists available at ScienceDirect

Algal Research

journal homepage: www.elsevier.com/locate/algal

From spores to gametes: A sexual life cycle in a symbiotic *Trebouxia* microalga

Ayelén Gazquez [a,1], César Daniel Bordenave [a,*,1], Javier Montero-Pau [a,*], Marta Pérez-Rodrigo [b], Francisco Marco [b], Fernando Martínez-Alberola [a], Lucia Muggia [c], Eva Barreno [a,2], Pedro Carrasco [b,2]

[a] Instituto Cavanilles de Biodiversidad y Biología Evolutiva (ICBiBE), Botánica, Universitat de València, C/Dr. Moliner, 50, 46100 Burjassot, Spain
[b] Inst. Univ. Biotecnología y Biomedicina (BIOTECMED), Universitat de València, C/Dr. Moliner 50, 46100 Burjassot, Spain
[c] University of Trieste, Department of Life Sciences, via L. Giorgieri 10, 34127 Trieste, Italy

ARTICLE INFO

Keywords:
Phycobiont
Terrestrialization
Chlorophyta
Microalgae
Whole genome sequencing
Sexual reproduction

ABSTRACT

Trebouxiophyceae are particularly widespread in terrestrial environments and comprise most of the lichen-forming microalgae genera. These symbionts have been frequently considered asexual, however, their life cycles remain largely unknown. We sequenced and analysed the nuclear genome of *Trebouxia lynniae*, a model Trebouxiophyceae phycobiont, monitored and modelled its colony proliferation and analysed cell population dynamics by using flow cytometry coupled with microscopy and ploidy analysis. The genome inspection unveiled the presence of a "meiosis toolkit", indicative of sexual reproduction, and the absence of TALE transcription factors related with haplontic life cycles. Moreover, we reveal that *T. lynniae* possesses a diploid genome, sexual reproduction, and diplontic life cycle. Also, we have demonstrated that its zoospores are gametes, and that meiosis is prezygotic. These discoveries illuminate Trebouxiophyceae ecology and evolution, highlighting the potential adaptive significance of sex in the face of challenging and changing ecological conditions like those faced by lichen symbionts. Moreover, characterizing this terrestrial Chlorophyta's life cycle contributes to shape evolutionary theories that aim to elucidate the path that they took during terrestrialization, suggesting that, as proposed for Streptophyta, it may have been mediated by a life cycle shift.

1. Introduction

Green plants are the dominant eukaryotic photosynthetic organisms across Earth's terrestrial landscape and since their evolution the biosphere changed drastically. Both Streptophyta and Chlorophyta have colonised terrestrial environments independently [1]. However, while Streptophyta terrestrialization has been extensively discussed, our understanding of Chlorophyta's adaptation to land remains largely forgotten [2]. Evolutionary theories state that Streptophyta transition to land entailed changes in their life cycle in which the diploid phase became dominant. In the case of Chlorophytes, most known life cycles belong to aquatic species, leaving the terrestrial counterparts unexplored [3]. Green algae colonization of land was most likely facilitated by fungal symbiosis [1], therefore extant lichens and their microalgal symbionts conceal key information about Chlorophyta evolution to terrestrial life. However, our understanding of proliferation and reproduction strategies of phycobionts remains limited [4–8]. Among Chlorophyta, Trebouxiophyceae is one of the largest classes, it includes most of microalgae reported as lichen symbionts, possess an extraordinary capacity to adapt to diverse environments and thrive in seemingly inhospitable habitats [9–11], and it is proposed as one of the first terrestrial plant lineages [2,3,9].

The closely related aeroterrestrial green algae genera *Trebouxia* Puymaly and *Asterochloris* Tschermak-Woes encompass the majority of species identified as lichen phycobionts [12,13]. Both genera consist of unicellular coccoid cells with an axial chloroplast that occupy a significant portion of the cell volume [14,15]. When axenically cultured they grow better in solid media, where they develop thick colonies resembling natural occurring biofilms (reviewed by [16]), than in liquid medium, where the alteration of their morphology results evident [14]. Only a few publications have focused on the development and the life

* Corresponding authors.
E-mail addresses: cesar.bordenave@uv.es (C.D. Bordenave), javier.montero@uv.es (J. Montero-Pau).
[1] These authors contributed equally to this work.
[2] Senior authors.

https://doi.org/10.1016/j.algal.2024.103744
Received 25 April 2024; Received in revised form 4 September 2024; Accepted 8 October 2024
Available online 12 October 2024

Abbreviations

BBM	Bold's Basal Medium
PAR	photosynthetically active radiation
GO	Gene ontology
IntDen	integrated density
NLS	Nonlinear Least Squares
DAPI	4′-6-diamino-2-phenylindole
PBS	phosphate-buffered saline
SSC-A	side scatter area
SSC-H	side scatter height
FSC-A	forward scatter area
CLSM	confocal laser scanning microscopy
TEM	Transmission electron microscopy
GMM	Gaussian Mixture Model
c-value	DNA content

cycle of these algae [7,8,13]. Depending on the species, the vegetative cell can generate varying proportions of autosporangia and zoosporangia. Autosporangia are characterised as clusters of cells known as autospores [8], which are smaller than the vegetative cells and develop into mature vegetative cells. Meanwhile, zoosporangia give rise to numerous small flagellated cells, known as zoospores [17], presumed to subsequently develop into autospores and eventually mature into vegetative cells. Overall, the life cycles documented so far have primarily assumed asexual reproduction.

Different pieces of information are considered evidence of sexual reproduction to a different extent. Genomic evidence, such as the presence of specific genes associated with meiosis and gamete fusion, serves as robust proof of actual or cryptic sexual reproduction [18–20]. This has been recently documented in the Trebouxiophyceae class [21,22]. Another indication of sexual reproduction is homologous recombination, which has been reported in *Trebouxia* [23]. At the cellular level, the observation of cells morphologically consistent either with zygotes or with gametes, *i.e.* naked motile cells [24], are frequently reported in Trebouxiales [22], thus providing modest yet noteworthy evidence of sexual reproduction. Although fusion of gametes is a strong evidence already reported in this order, some authors did not distinguish between gametes and zoospores or questioned the sexual nature of this phenomenom [22]. Lastly, changes in nuclear ploidy levels, which suggest a reductional cell division, can also offer insights into the presence of sexual reproduction and meiosis [25]. The induction of sexual reproduction often depends on specific growth conditions and may occur during a particular growth phase [26]. Thus, it is crucial to test suitable growth conditions and describe the kinetics of different cell populations.

We hypothesised that sexual reproduction occurs in species of Trebouxiophyceae, supported by presence of meiotic genes, potential gamete cells, homologous recombination, and cell fusion. In this study, we investigated this hypothesis on *Trebouxia lynniae* Barreno grown as colonies on solid medium. We choose *T. lynniae* because it has been proposed as an ideal phycobiont model species [27] due to its comprehensive characterization [28,29], extensive research on its physiological responses to various conditions [30–41] and the sequencing of its chloroplast and mitochondrial genomes [42,43]. Here we sequenced its genome and tested it for the presence of specific genes related with sexual reproduction and meiosis. We also identified different stages of the life cycle using flow cytometry along with microscopy techniques. Reductional cell division was evaluated by following changes in DNA content during colony growth. Our study shows that *T. lynniae* has a diplontic sexual life cycle with isogamous gametes.

2. Material and methods

2.1. Microalga strain and growth conditions

Trebouxia lynniae was isolated in 2006 from a thallus of the lichen *Ramalina farinacea* collected from Sierra del Toro (39°57′ 32.34″N–0°46′ 35.51″W, Castellón, España) and the unialgal culture was stored and maintained as living culture at the Symbiotic Algal collection from the University of Valencia (https://www.asuvalgae.com/; ASUV44). Cultures were kept on 1.5 % agar Bold's Basal Medium (BBM) [44] in a growth chamber at 20 °C, with a 12 h photoperiod of 25 μmol photons m^{-2} s^{-1} of photosynthetically active radiation (PAR). Molecular identification has been routinely checked by means of internal transcribed spacer (ITS) amplification and sequencing as described by Barreno et al. [28].

In this research, two 3NBBM [45] supplemented mediums were used: GC-3NBBM, a 3NBBM medium with glucose 20 gL^{-1} and casein hydrolysate 10 gL^{-1}; 2GC-3NBBM, a 3NBBM medium with glucose 40 gL^{-1} and casein hydrolysate 20 gL^{-1}. At 21 days, entire colonies were scraped from agar medium, resuspended in GC-3NBBM or 2GC-3NBBM solution and filtered through a 50 μm pore filter (Partec; Celltrics). Filtered cells were counted in Neubauer's chamber and adjusted to 5.0×10^7 cells/mL. Filtered cell suspensions from three colonies were pooled together, analysed by flow cytometry and used as starting material in all experiments. 50 μL of filtered cell suspension were applied directly over solid GC-3NBBM or 2GC-3NBBM. Colony measurements and samples collection were done between 2 and 4 h after the light period started for consistency.

2.2. Genome sequencing, assembly and annotation

T. lynniae DNA library was sequenced using Illumina MiSeq (Illumina, San Diego, USA). *De novo* assembly was performed with Velvet v1.1 [46]. Genome quality and completeness was assessed by QUAST v.5.2.0 [47] and BUSCO v.5 [48]. Ploidy level was estimated with nQuire [49]. Structural annotation was performed using SNAP [50] and Augustus v.3.4.0 [51]. Functional annotation was assessed by BlastP, Gene ontology (GO), KEGG orthology and PFAM annotation. "Meiosis toolkit" genes and TALE homeobox family genes were selected and analysed based on specific references [18,19,52–59]. Details of the search method are available as supplementary material within Note S1.

Extended description of genome sequencing and annotation methods are available as Note S1.

2.3. Colony growth measurements

Colony growth was analysed using a photographic, non-destructive method that allowed us to follow each individual colony over time. Colonies growing on Petri plates were placed on a drawing table with integrated illumination and photographed in a dark room. This illumination method ensured optimal, uniform and controlled lighting while minimising shadows and reflections. Images were taken at fixed distance with a Canon EOS 2000D digital camera (Canon, Ōta City, Tokyo, Japan). To calibrate and standardise colour and size information during image processing and analysis a colour and a size scales were incorporated into the drawing table setup. Images were analysed with Fiji distribution of ImageJ v.1.53 [60] and morphological variables were acquired for each image of each colony. Briefly, for each colony the image was split into red, green and blue channels. Auto Threshold using Huang method was applied over the blue channel in order to segment the colony area. Green channel was used to segment the background applying an Auto Threshold using Huang method after transforming the image with a Gaussian Blur and a Median filter. The morphological variables acquired were area and integrated density (IntDen). The measurements were performed for the colony and the background regions in each, red, blue and green channels and the RGB image.

Data analysis was performed using R-Studio v.2022.02.0 [61] and R v.4.1.2 statistical software packages [62]. Data manipulation was done with *readr* v.2.1.4, *dplyr* v.1.1.2, *stringr* v.1.5.0 and *tidyr* v.1.3.0 packages [63–66]. For each measurement of area and IntDen the corresponding background value was subtracted from the colony value and data tables were prepared for fitting individual growth curves. Area or IntDen values were then used for fitting three parameter logistic least square growth curve models using the *minpack.lm* v.1.2–3 package [67]. The model is given by the following equation:

$$y = k/(1 + exp(-r^*(t - t_{mid}))),$$

where y is area or IntDen at time t; k is the carrying capacity of the population, the maximum colony size; t_{mid} is the time at which colony reaches half of its maximum size; and r is the intrinsic growth rate. For initial guessing of parameter values, k was assumed to be near the maximum of the data set, and initial slope r and t_{mid} were estimated from coefficients of a linear regression on pseudo y values. The pseudo y values were calculated as the logarithmic transformation of the difference between the carrying capacity and the observed value. The logarithmic transformation is used because it makes the data more linear near the carrying capacity. The slope of this linear regression was used as r initial value while t_{mid} was calculated as the quotient of the y-intercept divided by the slope. The initial values for k, r, and t_{mid} were used as starting values for the Nonlinear Least Squares (NLS) fit. The NLS fit then refines these values to find the best fit to the data. After curve fitting was performed, maximum growth rate (μm) was calculated as the slope at the midpoint as $r^*k/4$, the duration of the lag phase (t_{lag}) was estimated as the time at which the line passing through (t_{mid}, $k/2$) with slope μm equals the initial inoculum $y = n_0$, and the time at which k was reached and the stationary phase initiates (t_{stat}) was determined as the line passing through (t_{mid}, $k/2$) with slope μm equals $y = k$. Individual curves were evaluated and original and predicted values were plotted with the *ggplot2* v.3.4.2 [68]. A two sided Student's *t*-Test was done for statistical comparison of growth parameters k, r, t_{mid}, μm, t_{stat} and t_{lag} between growth mediums, homoscedasticity and normality were tested. Besides, r for data points at $t_i > t_{lag}$ was estimated as $\ln(\text{IntDen}(t_2)/\text{IntDen}(t_1))/(t_2 - t_1)$, where t_2 and t_1 are two contiguous time points $t_2 > t_1$.

2.4. Cell fixing and nuclear staining

Cell fixing and nuclear staining was based on Ulrich & Ulrich [69] and Čertnerová [70]. Each sample consisted of three colonies harvested with a microbiological loop and mixed with cold 3:1 *v*/v absolute ethanol:acetic acid with Tween 20 for fixing and clearing. Samples were counted with an hemocytometer and kept at 4 °C for a period ranging from 24 h up to several weeks before use. Sample concentration was adjusted and then either directly analysed by flow cytometry or nuclear stained. For nuclear staining, 4′-6-diamino-2-phenylindole (DAPI, Invitrogen) was used according to the manufacturer. Briefly, cell suspension of 7.5×10^5 cells was collected, centrifuged 5 min at 8000*g* and the supernatant discarded. Cells were resuspended in 1 mL phosphate-buffered saline (PBS) and incubated 20 min at room temperature for rehydration. After centrifugation for 5 min at 8000*g*, supernatant was discarded and cells were incubated with 500 μL of 10 μg mL^{-1} DAPI in PBS (1×10^{-6} μg DAPI x $cell^{-1}$). After 30 min in darkness, the suspension was centrifuged 5 min at 8000*g*, supernatant was discarded and cells were resuspended in PBS buffer and analysed immediately by flow cytometry and confocal microscopy.

Following cell staining, the intensity of fluorescence integrated over the analysed cells is expected to be in stoichiometric relationship to DNA content, and thereby can be used to determine relative DNA content. For this, the peak with the lowest DAPI intensity was considered 1c and the intensity for the other ploidies were calculated by multiplying 1c intensity with the corresponding factor (*i.e.* 2*1c for 2c, 4*1c for 4c, and so on).

2.5. Flow cytometry and cell sorting

For flow cytometry, entire colonies were scraped from agar medium, resuspended in 500 μL of GC-3NBBM, 2GC-3NBBM or fixing solution for DNA staining. Fresh samples were analysed immediately after being collected. Resuspended colony samples were filtered through a 50 μm pore filter (Partec; Celltrics), injected in a LSR-Fortessa cytometer (Becton, Dickinson and Company, BD, USA) with 488 and 405 nm lasers and data was recorded until the least abundant population reached 10,000 events. Every sample was manually inspected for early anomalies (Fig. S1). Cell populations were gated initially by size (forward scatter area; FSC-A) and chlorophyll autofluorescence using the BV650-A filter (670/30), and then single cells were discriminated within each population by side scatter area (SSC-A) and side scatter height (SSC-H) discordance (Fig. S1). For DAPI staining, all samples were stained, kept in darkness till injected in the cytometer and analysed on the same day in a random order to minimise procedure error and equipment variation due to maintenance and recalibration. DNA was measured using the Indo-1 (violet) filter (450/50) and populations were gated by means of Indo-1 (violet)-A. Cells bearing a single nucleus were discriminated for each population by Indo-1 (violet)-A and Indo-1 (violet)-H discordance (Fig. S1). Some samples were kept and used as comparison between experiments analysed in different dates. The equipment configuration was recorded and kept constant for all experiments.

Flow cytometry data analysis was carried out using the *CytoExploreR* v.1.1.0 [71]. For cell population frequency calculations, population profiles over time were modelled by local polynomial regression using LOESS with the geom smooth function from the *ggplot2* v.3.4.2.

For cell sorting, entire colonies were scraped from the agar medium, resuspended in 500 μL GC-3NBBM or 2GC-3NBBM solution and filtered through a 50 μm pore filter (Partec; Celltrics). The filtered cell suspensions were injected in a BD FACSAria Fusion platform (Becton, Dickinson and Company, BD, USA). Chlorophyll autofluorescence signal was acquired using the 650 nm filter after excitation by means of the 488 nm laser. Populations were gated based on chlorophyll autofluorescence using the BV650-A filter (670/30) and size (FSC-A). Single cell populations within each group were discriminated from grouped cells by SSC-A and SSC-H discordance (Fig. S1). The sorted populations were collected in fresh GC-3NBBM or 2GC-3NBBM liquid medium or fixing solution until the least abundant population reached 10,000 events. Sorted populations were always inspected by light microscopy. Filtered samples used for cell sorting were also injected in an LSR-Fortessa cytometer (Becton, Dickinson and Company, BD, USA) and results were compared to those obtained with the cell sorter. When used for confocal laser scanning microscopy (CLSM), the sorted populations were centrifuged for 5 min at 13,000 rpm and the pellet was resuspended in 30 μL of fresh medium and used as specified below. The remaining sample was plated in fresh medium to observe viability. The sorting and identification of cell populations was repeated at least three times in independent experiments for each of the analysed time points.

Quality control of the Cytometry equipment was performed periodically over the year, each year, during the experiments duration (Data S1).

2.6. Microscopy

For CLSM 15 μL of each sample were placed on plates with a thin layer of 1 % agar in sterile water, air dried and placed upside down over a 35 mm imaging dish suitable for inverted microscopy (Ibidi, Fitchburg, WI, USA). An Olympus FLUOVIEW FV1000 laser scanning confocal microscope (Olympus, Tokyo, Japan) was used with a 405 nm excitation laser. Fluorescence emitted from 650 to 750 nm was collected to observe chlorophyll autofluorescence, thus recovering the chloroplast layers.

For DAPI staining, the same procedure was followed with

modifications. Samples were kept in darkness until analysed and a Zeiss LSM 980 confocal microscope (Carl Zeiss, Jena, Germany) was used, with a 405 nm excitation laser [72]. Fluorescence emitted from 650 to 750 nm was collected to observe chlorophyll autofluorescence, and from 408 to 550 nm was collected to observe DAPI staining. Image acquisition parameters were kept constant for all DAPI experiments. No stained controls were always included in the analyses (Fig. S2).

For cell-wall staining, the same procedure was followed with modifications. Samples were kept in darkness, and treated with a droplet of Calcofluor white solution (1 g/L) for 1 min, followed by a droplet of 10 % KOH. Afterwards samples were placed upside down over a 35 mm imaging dish suitable for inverted microscopy (Ibidi, Fitchburg, WI, USA). An Olympus FLUOVIEW FV1000 laser scanning confocal microscope (Olympus, Tokyo, Japan) was used with a 405 nm excitation laser. Fluorescence emitted from 650 to 750 nm was collected to observe chlorophyll autofluorescence, and from 450 to 480 nm was collected to observe Calcofluor white staining.

Series of images were captured with a separation of 0.4 μm. The image stacks were preprocessed to remove noise and then analysed using the z-projection tool and volume viewer with Fiji distribution of ImageJ v.1.53. Transmitted light channel was processed with the Stripes Filter tool from the Xlib plugin [73]. For DAPI intensity estimation, whole cells or nuclei were manually segmented over the max z-projected image followed by measurement of the region intensity.

For Transmission electron microscopy (TEM) analyses, a portion of the sample of the microalgal colony of about 2 × 2 mm was covered with tempered 1 % low melting point agarose and processed following fixation and dehydration protocols as described in Bordenave et al. [29]. Sections were observed at 80 kV under a JEOL JEM-1010 microscope (Jeol, Peabody, MA, USA). Images were obtained using an Olympus MegaView III camera and processed with the Fiji distribution of ImageJ v.1.53.

2.7. Experimental design

Preliminary experiments (Fig. S3a). To set up and optimize experimental measurements, colonies growing in GC-3NBBM or 2GC-3NBBM were analysed by flow cytometry and populations were sorted and inspected by LSCM for identification. Additionally, another set of samples were sorted, fixed and analysed by flow cytometry for comparison with fresh samples. An aliquot of each fixed population was DAPI stained and analysed by flow cytometry and LSCM for characterizing each population relative DNA content.

Main experiments (Fig. S3b). A total of eight independent experiments were carried out. Four experiments with colonies growing in GC-3NBBM and four in 2GC-3NBBM. All the experiments were followed by non-destructive photography to assess colony proliferation, with at least ten samples per time point. Two experiments in each condition were also followed by flow cytometry of fresh colonies, with at least three samples per time point. Two experiments in each condition were followed by flow cytometry of fixed colonies, with at least three samples per time point. These fixed samples were also used for relative DNA content estimation by DAPI staining and flow cytometry.

3. Results

3.1. Genomic ploidy and meiotic genes suggest sexual reproduction

The *de-novo* assembly of *T. lynniae* genome resulted in a 59,411,922 bp size, with a contig N50 of 242,042 and 274 contigs of more than 50 Kb. The genome is predicted to contain 15,742 protein-coding genes, with an average gene length of 2267 bp (Table 1, Note S2, Data S2). To estimate genome ploidy, the distribution of allelic frequencies of SNPs after mapping genomic reads against the genome was explored. This distribution shows a peak at 50 % frequency compatible with a diploid genome (Fig. 1a, Fig. S4). Although the Gaussian Mixture Model (GMM), as obtained with nQuires, supports a tetraploid genome over a diploid one (Δlog-likelihood between a free parameter GMM and tetraploid and diploid models was 412.7 *vs.* 3377.5, respectively, suggesting a better fit to a tetraploid model) this could be affected by the extremely low level of heterozygosity of the genome (0.063 % of global heterozygous as inferred by k-mer analysis).

Comparative analysis with other Trebouxiophyceae microalgae revealed a genome size in the range of other species and comparable structural features (Fig. 1b, Table S1, Fig. S4). A total of 1666 orthologs were shared among the 8 species from different phylogenetic lineages, while 539 were unique to *T. lynniae* (Table S1 and Data S3). GO terms could be assigned to 15,298 protein-coding genes (94.2 % of the total) and KEGG terms to 6204 (34.4 %, Fig. 1c). The enriched functional categories highlighted basic functions such as carbohydrate metabolism or biological regulation which is consistent with most genome functional descriptions (Fig. 1c, Note S2, Figs. S5–8).

In recent decades, a consensus has emerged regarding the significance of a core set of sex and meiosis genes, known as the “meiosis toolkit”, in determining an organism's ability to undergo sexual reproduction. We conducted a comprehensive analysis by combining the genes identified in 10 studies, resulting in a total of 26 genes belonging to the “meiosis toolkit”. Through an examination of the genome of *T. lynniae* using profile hidden Markov models, and employing sequence alignment and phylogeny reconstruction to discriminate between meiosis genes and their paralogs (Figs. S9–19, Data S4), we successfully identified 22 out of the 26 genes (Fig. 1d, Table S2). The expression of these genes was compared to the whole transcriptome, and to genes considered to be housekeeping, in order to corroborate that they are expressed but not constitutively (Fig. S20). These findings strongly suggest that *T. lynniae* possesses the capability for sexual reproduction.

Meiosis can be pre or post zygotic. In haploid plants, the haploid gametophyte produces haploid gametes that fuse into a diploid pre-meiotic spore (zygospore). In diploid (or diploid dominant) plants, the diploid zygote forms a diploid sporophyte which in time produces postmeiotic haploid spores. These patterns are governed by the TALE homeobox family of transcription factors [74]. We inspected the *T. lynniae* genome and transcriptome for homeobox proteins and only retrieved a single homeobox sequence (Data S5) that does not belong to the TALE homeobox family (Data S4).

3.2. Cell profiling pattern changes under different growth conditions

Within the described cell populations of *T. lynniae* [28], we considered that cells identified as zoospores had characteristics that align with the general attributes of algal gametes, namely motility (*via* flagella) and the absence of a cell wall [24]. To avoid making assumptions about the nature of these cell types, from now on we will refer to them as

Table 1
Trebouxia lynniae nuclear genome statistics.

Total length	59,411,922
# contigs	1892
# contigs (≥1000 bp)	579
# contigs (≥50,000 bp)	274
Largest contig	1,171,635
N50	242,042
N90	64,425
L50	74
L90	245
# Ns for 100 Kb	642.67
# Predicted protein-coding genes	15,742
Average gene length	2267.2
Average # of exons	3.94
Gene density per Kb	0.26
Completeness BUSCO (%)	93.7
k-mer estimated genome size (bp)	57,548,506
k-mer estimated heterozygosity (%)	0.0626
k-mer estimated read Error Rate (%)	0.123102

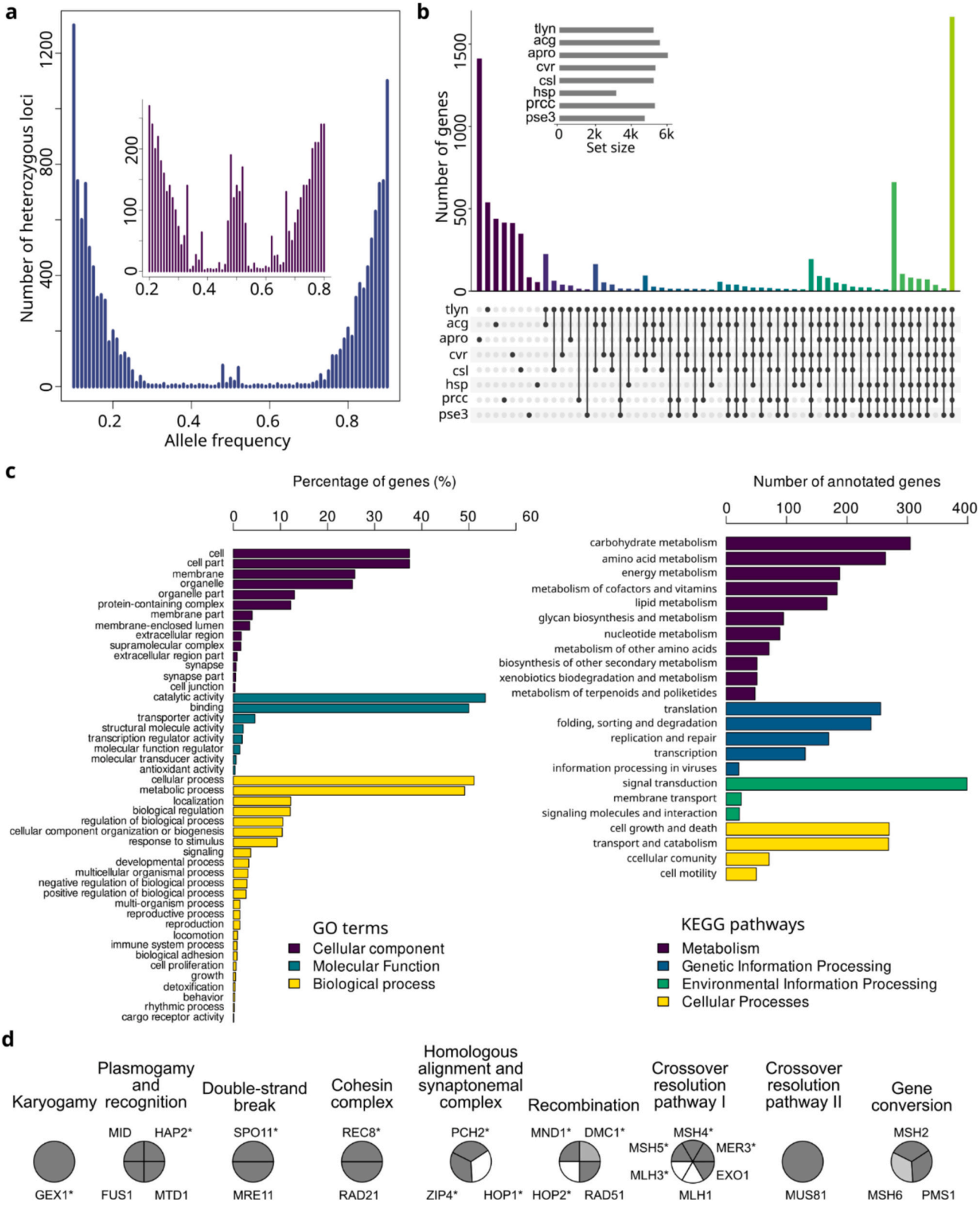

Fig. 1. Nuclear genome and "meiosis toolkit" of *Trebouxia lynniae*. (a), Allelic frequency distribution observed for all scaffolds. (b), UpSet graph showing the number of genes shared in each possible combination of the eight compared genomes. The size of each genome is indicated in the inset and abbreviations correspond as follows: tlyn, *Trebouxia lynniae*; acg, *Asterochloris glomerata* Cgr-DA1pho v2.0; apro, *Auxenochlorella protothecoides*; cvr, *Chlorella variabilis* NC64A; csl, *Coccomyxa subellipsoidea* C-169; hsp, *Helicosporidium* sp.; prcc, *Picochlorum* RCC4223; pse3, *Picochlorum* sp. SENEW3. (c), GO and KEEG functional annotation of *T. lynniae* nuclear genome. (d), "Meiosis toolkit" genes detected in the nuclear genome of *T. lynniae*; dark grey filled areas indicate the presence of at least one copy of the gene, light grey indicates partial sequence or unsolved gene phylogeny, white filled areas indicate absence. Gene names followed by an asterisk indicate genes specific to meiosis and sexual reproduction.

flagellated cells as their identity remains unclear.

T. lynniae is usually grown in a modified BBM medium supplemented with glucose and casein (GC-3NBBM) as this allows the observation of all known cell types [28], although flagellated cells are still difficult to find. We used double the amount of casein and glucose (2GC-3NBBM) to test if flagellated cells production may be enhanced. To accurately quantify the production of flagellated cells we employed flow cytometry measurements. Therefore, a combination of cell sorting and CLSM was used to identify cell populations present in a colony. We discriminated cell populations with the flow cytometer based on cell chlorophyll autofluorescence and size. Based on the morphological traits [14,28,29] observed with the CLSM we categorised these cell populations into four main groups (Fig. 2a, b, Fig. S21). Young cells are spherical vegetative cells, measuring 4–9 μm in diameter, with a shallowly lobed chloroplast. Mature cells encompass two subpopulations: one consists of spherical vegetative cells of 9–11 μm with a shallowly lobed chloroplast, and the other consists of slightly bigger cells of 12–14 μm showing a chloroplast with small lobes over the shallow lobes, resulting in a curly lobed chloroplast. The group of dividing cells includes cells undergoing chloroplast division of 7–9 μm, as well as sporangia of 11–18 μm which contain a varying number of spores, either with a cell wall or naked. The flagellated cells population comprises slightly pyriform cells of 5–7 μm at their major diameter. They lack a cell wall, possess two flagella and contain a globular chloroplast.

Colony proliferation was monitored using a non-destructive photographic method where IntDen was used as a measure of proliferation (Fig. 2c). IntDen was preferred over colony area (Fig. S22) as it is more sensitive to small population changes and accounts for vertical expansion of the colony as well as horizontal growth. The algae growing in the GC-3NBBM medium showed both the lag phase and the exponential phase to be shorter than those of 2GC-3NBBM (Table S3). As expected, the carrying capacity (k) was higher in the nutrient-rich medium; however, no differences were found in the maximal growth rate (μ_m) estimated from the adjustment to the logistic model of the set of dynamics. This is because, contrary to what is expected, the global fitted intrinsic growth rate (r) was higher in the nutrient-poor environment than in the enriched one.

We monitored the frequency of the four cell populations during colony proliferation in each medium (Fig. 2c). Young cells constituted the majority of events during the whole analysed time in the GC-3NBBM medium. Mature cells and dividing cells remained constant during the studied period, but at lower frequencies. Flagellated cells showed a slight increment during the exponential phase but reached a low frequency. In contrast, colonies cultivated in 2GC-3NBBM evidenced great changes in the boundaries of growth phases. Although the frequency of young cells was the highest in the lag phase, it dramatically decreased when entering the exponential phase. Dividing cells started at lower frequencies than young cells, but as colonies entered the exponential phase they became the most abundant population. The transition to the stationary stage was marked by a drop in the frequency of dividing cells and a significant increase in flagellated cells which were almost undetectable in previous stages. Mature cells stayed at low frequencies throughout the whole experiment. The shift between cell types in *T. lynniae* colonies was found to be a gradual process, as observed through the scatter plots during colony proliferation (Figs. S23, S24, Videos S1, S2). The boundaries surrounding, and between, different cell populations appeared to be diffuse and challenging to establish. This suggests that the transition between cell populations is not sharply defined but rather occurs gradually, with cells exhibiting intermediate characteristics between different stages.

Our data suggest that the investment in flagellated cells could be the result of local density-dependent cues. Moreover, when inspecting individual growth curves, the r in both culture media were similar before the production of flagellated cells began, but an important decrease in r occurred in the rich medium coinciding with the high investment in flagellated cells (Fig. 2c). As a result, the global fitted r was lower. This is the result of diverting resources previously used for vegetative growth into producing sexual gametes (*i.e.*, demographic cost of sex; [75]).

3.3. *Trebouxia lynniae flagellated cells are gametes*

Sexual reproduction in *T. lynniae* would imply that a meiotic phenomenon should occur, mainly characterised by a reductional division where chromosome number goes from diploid to haploid [25]. To verify if flagellated cells are a product of prezygotic reductional division, we tested the relative DNA content (c-value) of individual cell populations at different times of colony proliferation. In order to do this, populations were sorted and fixed, DNA was stained with DAPI and samples were analysed using flow cytometry (Fig. 3a). In this way we were able to compare scatter plots of fresh and fixed samples. The fixation process reduced chloroplast autofluorescence but still allowed for the continuous monitoring of cell population frequencies. This enabled the establishment of new gating strategies for fixed cell populations. Uninucleated events showed that the peak with the lowest DAPI intensity in the whole sample (1c DNA content) was exclusive to flagellated cells population. Young and mature cells exhibited different frequencies of 2c, 3c, and 4c peaks. It is likely that 2c and 4c correspond to G1 and G2 cell cycle phases, respectively, while 3c corresponds to S phase. Dividing cells population displayed a low frequency of events with 3c, and a majority of events of 4c or higher peaks, as expected for multinucleated structures.

When fixed whole samples were analysed, events corresponding to 1c relative DNA content were exclusively located in the scatter plot region corresponding to flagellated cells throughout the entire duration of the proliferation curve in both growth mediums (Fig. 3b). Moreover, the increase in frequency of cells with 1c relative DNA content coincided with the increase in frequency of flagellated cells, whether grown under GC-3NBBM or 2GC-3NBBM conditions (Fig. S25, S26).

To validate relative DNA content estimation, microscopy analyses were performed on fixed samples of colonies growing exponentially in 2GC-3NBBM, so that all cell populations could be found and flagellated cells were abundant. Quantification of DAPI intensity in sorted cell populations using image analysis yielded relative DNA content profiles and stoichiometry similar to those obtained by flow cytometry (Fig. 3c, d). The analysis revealed that most young cells displayed a 2c relative DNA content, while mature cells exhibited a range of relative DNA content from 2c to 4c. Flagellated cells were predominantly observed with 1c relative DNA content, although a minority had 2c relative DNA content. The occurrence of cells with 2c relative DNA content in this gated population can be explained by multiple factors, such as the slight overlapping with young cells when fixed or the existence of zygotes within this population.

While flagellated cells had intense plastidial DNA, vegetative cells showed a diffuse DAPI fluorescence background (Fig. 3c). Hence, an image analysis was performed in which the nuclei were segmented, and nuclear DAPI staining was estimated ($n = 6$). This analysis resulted in a nuclear DAPI IntDen of 1580 ± 890 for flagellated cells, 3180 ± 750 for young cells, and 6770 ± 384 for mature cells, corresponding stoichiometrically to 1c, 2c, and 4c, respectively. All in all, we conclude that 1c naked flagellated cells can be classified as gametes and they are a product of a reductional division. Moreover, no evidence was found supporting the existence of 1c vegetative cells.

3.4. *The diplontic life cycle of Trebouxia lynniae*

We further examined the flagellated cells population to find empirical evidence of events related with sexual reproduction and mating. Microscopic examination of whole samples with abundant gametes, or freshly sorted flagellated cells, revealed various stages of the mating process (Fig. 4a). The initial step involves recognition and contact, where a fertilization tube is extended [76], followed by flagellar adhesion and plasmogamy. After cell fusion, a tetra-flagellated zygote is

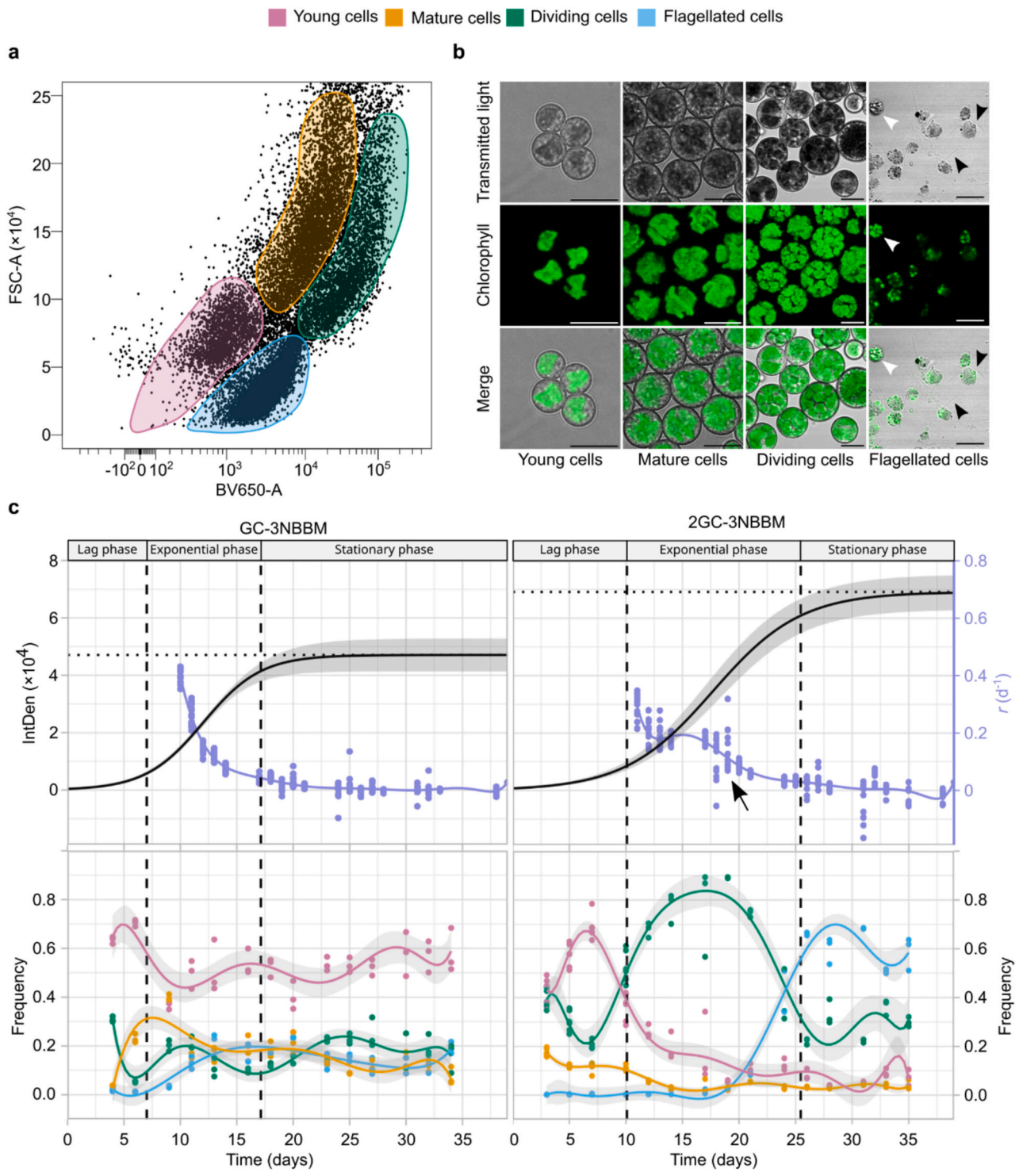

Fig. 2. Identification and profiling of cell populations during colony growth of *Trebouxia lynniae*. (a), Gating strategy of the four main cell populations over a scatter plot of chlorophyll autofluorescence *vs* cell size of a 30 d sample grown on 2CG-3NBBM. (b), CLSM max z-projection of chlorophyll autofluorescence of cell populations sorted following the gating strategy displayed in Fig. 2a. Black arrowheads indicate flagella, white arrowheads indicate putative zygotes. Scale bars = 10 μm. See Fig. S21. (c), Representative growth curves and cell population profiling (out of two fully performed experiments). Upper graphs display growth curves as the integrated density (IntDen) *vs* days of growth (Time): solid black line represents average predicted value of models ($n = 15$), grey areas show s.d. 95 % confidence interval; intrinsic growth rate (r) original data points ($n = 15$) after lag phase (t_{lag}) are shown in violet, to aid pattern visualization a smooth was performed with a generalised additive model; point-lines indicate the final size of the colony (k), dashed lines indicate the start (t_{lag}) and the end (t_{stat}) of the exponential growth phase (see Table S3 for mean ± s.d. of growth parameters); a black arrow points to the additional decrease in r. The graphs at the bottom display cell populations profiling as the frequency *vs* days of growth. Original data points are shown ($n = 3$), to aid pattern visualization a smooth was performed with linear modelling y ~ poly(x, i), where $i = 7$ for CG-3NBBM and $i = 9$ for 2CG-3NBBM, s.d. 95 % confidence interval is shown in grey. (For interpretation of the references to colour in this figure legend, the reader is referred to the web version of this article.)

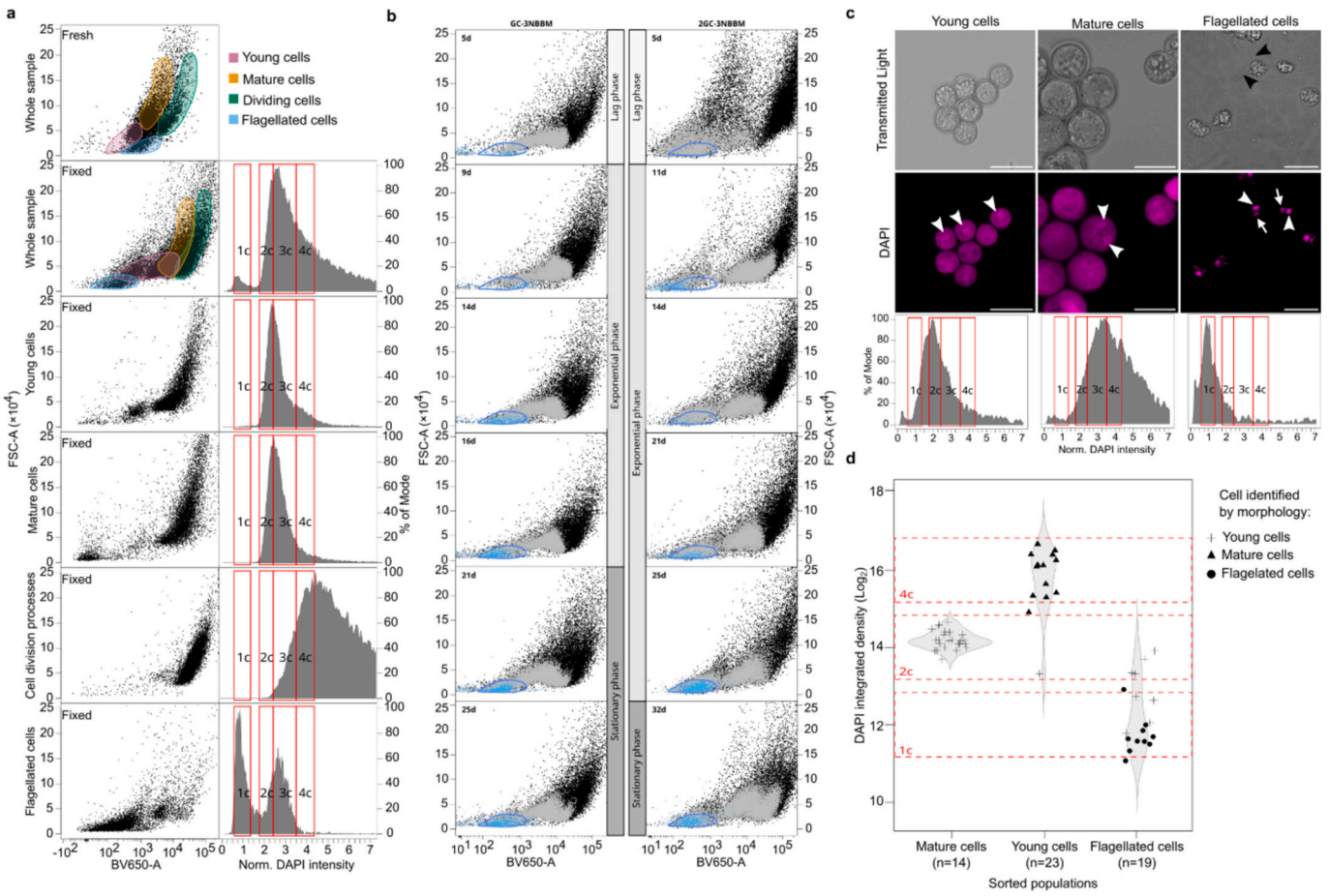

Fig. 3. Characterization of relative DNA content of cell populations of *Trebouxia lynniae*. (a), Representative sample ($n = 4$) of CG-3NBBM of 30 d of growth. Scatter plots of chlorophyll autofluorescence *vs* cell size on the left panels. Histograms of DAPI stained samples displaying relative ploidy level on the right panels. (b), Representative scatter plots ($n = 3$) of chlorophyll autofluorescence *vs* cell size of one representative sample per time and medium of growth (CG-3NBBM and 2CG-3NBBM). Two full experiments were performed. Light blue dots indicate 1c relative ploidy level of uninucleate events, the rest of uninucleate events are marked in grey and the rest of the sample is indicated in black. Areas encircled in blue correspond to flagellated cell gating. Vertical grey bars indicate if the sample belongs to the lag, exponential or stationary phase based on Fig. 2c. (c), Sample of 2CG-3NBBM grown for 17 d. CLSM Max z-projection of DAPI stained sorted populations. DAPI histograms of each population are shown. Black arrowheads indicate flagella, white arrowheads show nuclei and white arrows show plastidial DNA. Scale bars = 10 μm. (d), Sample of 2CG-3NBBM grown for 17 d, same as in Fig. 3c. Estimation of relative DNA content by image analysis of DAPI stained sorted populations. Different symbols indicate the cell type identified by cell morphology (based on size, cell wall and flagella). Red dashed lines delimit boxes of different ploidy levels. (For interpretation of the references to colour in this figure legend, the reader is referred to the web version of this article.)

formed (Video S3). Interestingly, sorted flagellated cells samples often showed co-occurrence of cells bearing cell wall (cell-walled zygotes) with the same chloroplast morphology as the gametes (Figs. 2b, 4b). Both tetra-flagellated and cell-walled zygotes were approximately twice the size of gametes. The presence of these mating stages in the flagellated cell population explains the 2c DNA peak observed above, and the measurements of 2c DNA cells in the microscopical observations (Fig. 3).

To further inquire into cell division processes of the life cycle, we explored whole colony samples. CLSM cell-wall staining (Fig. 4b) and TEM (Fig. 4c) of sporangia revealed the presence of two distinct sporangia types. The first one consists of a symmetric sporangium, known as autosporangium, where daughter cells (4 to 32; [28]) have a cell wall (Video S4). The first stages of autosporangium development consist of plastid symmetric divisions followed by cytokinesis and deposition of the cell wall. This sporangium envelope tends to remain attached to daughter cells after their release. The other type are asymmetric sporangia that contain naked flagellated gametes (Video S5), previously termed zoosporangium. In light of the new evidence presented here, we propose to call it, from hereon, gametangium. The first stages of gametangium development consist of multiple asymmetric plastid divisions into small globular structures followed by cytokinesis (Fig. 4d). Gametangium releases gametes as a pack through a single narrow opening (ostiolum; Video S6).

Based on the collective evidence derived from genome analysis, cell population characterization, growth conditions, microscopy observations, relative DNA content analysis and, in particular, the absence of populations other than flagellated cells with 1c relative DNA content, we propose a diplontic sexual life cycle for *T. lynniae* (Fig. 5). Asexual reproduction of this species starts with a chloroplast and nuclear mitotic division, and continues with the formation of an autosporangium that contains small diploid vegetative cells with a developed cell wall. When young vegetative cells are released, some of them can stay attached to the mother cell wall. The fully developed mature vegetative cells start the cycle over again. The sexual part of the cycle initiates with meiotic reduction and nuclear division of the mature cell and multiple chloroplast divisions. The asymmetric gametangium matures with the development of cell membranes and flagella of new gametes. The gametangium then releases these gametes through an ostiolum and they undergo mating through recognition, contact, flagellar adhesion, plasmogamy and eventually karyogamy, leading to the formation of tetra-flagellated zygotes. Finally, zygotes become mature vegetative cells by fully developing the chloroplast and cell wall.

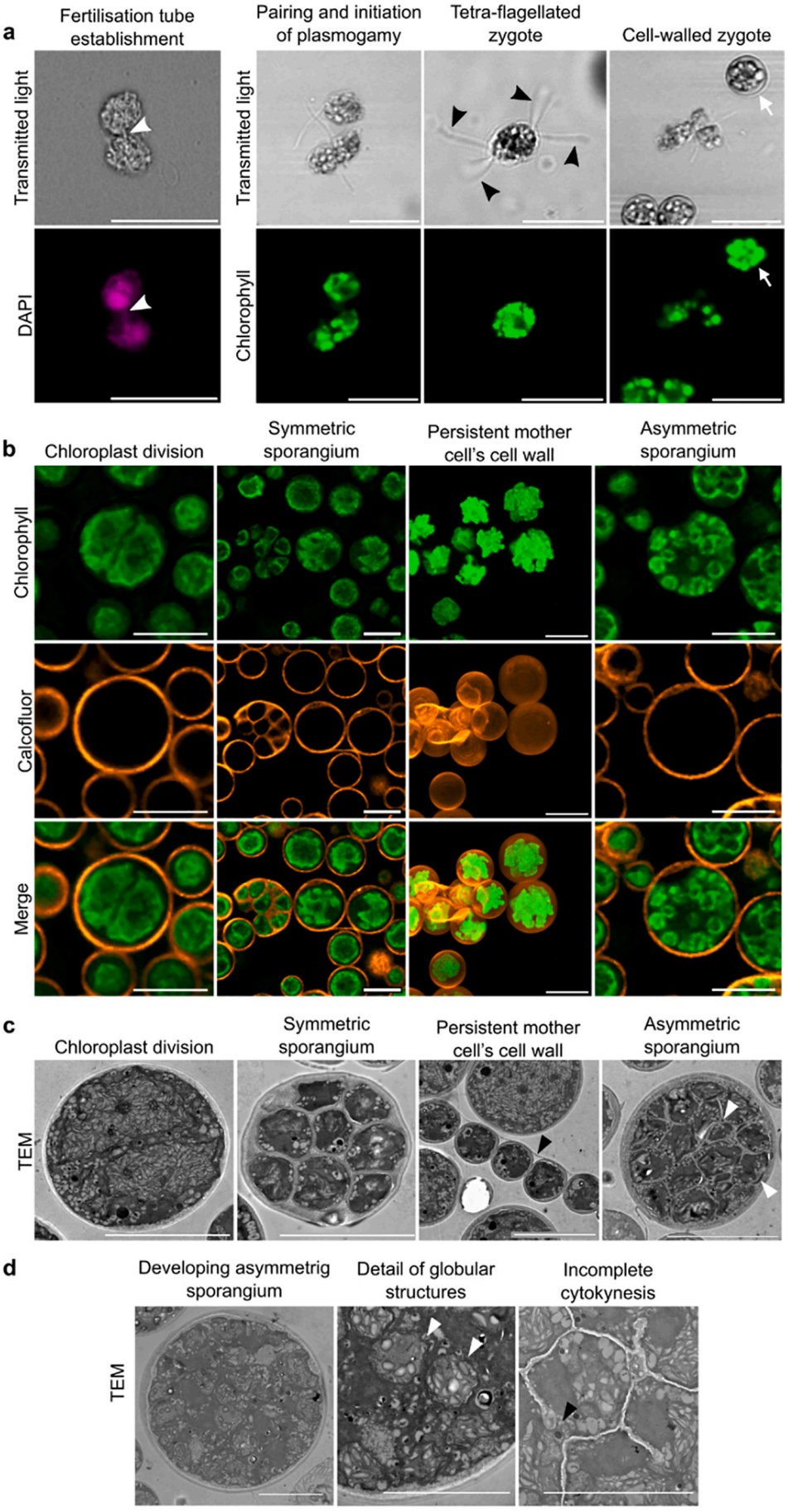

(caption on next page)

Fig. 4. Microscopic evidence of *Trebouxia lynniae* life cycle events. (a), Representative pictures of DAPI stained whole samples or sorted flagellated cells of a 21 d 2GC-3BBN sample ($n = 3$). CLSM max z-projection of different stages of sexual reproduction are shown. Events were observed at least 10 times with the exception of the fertilization tube and the tetra-flagellated zygote that are difficult to find because of their short life nature. White arrowheads indicate the fertilization tube, black arrowheads indicate flagella and white arrows show the cell-walled zygote. Scale bars = 10 μm. (b), Representative pictures of a fresh 21 d 2GC-3BBN sample stained with calcofluor for cell wall observation ($n = 3$). CLSM slice pictures of chlorophyll and calcofluor are shown in all cases, except for the one exemplifying the persistent mother cell's cell wall which corresponds to a max z-projection. Scale bars = 10 μm. (c), TEM micrograph of a 21 d 2GC-3BBN sample ($n = 3$) showing different sporangia and stages. Black arrowhead indicates persistent mother cell's cell wall and white arrowheads indicate flagella. Scale bars = 10 μm. (d), TEM micrograph of the same sample as in Fig. 4c showing details of asymmetric sporangium development. White arrowheads indicate globular structures and the black arrowhead shows an incomplete cytokinesis. Scale bars = 5 μm.

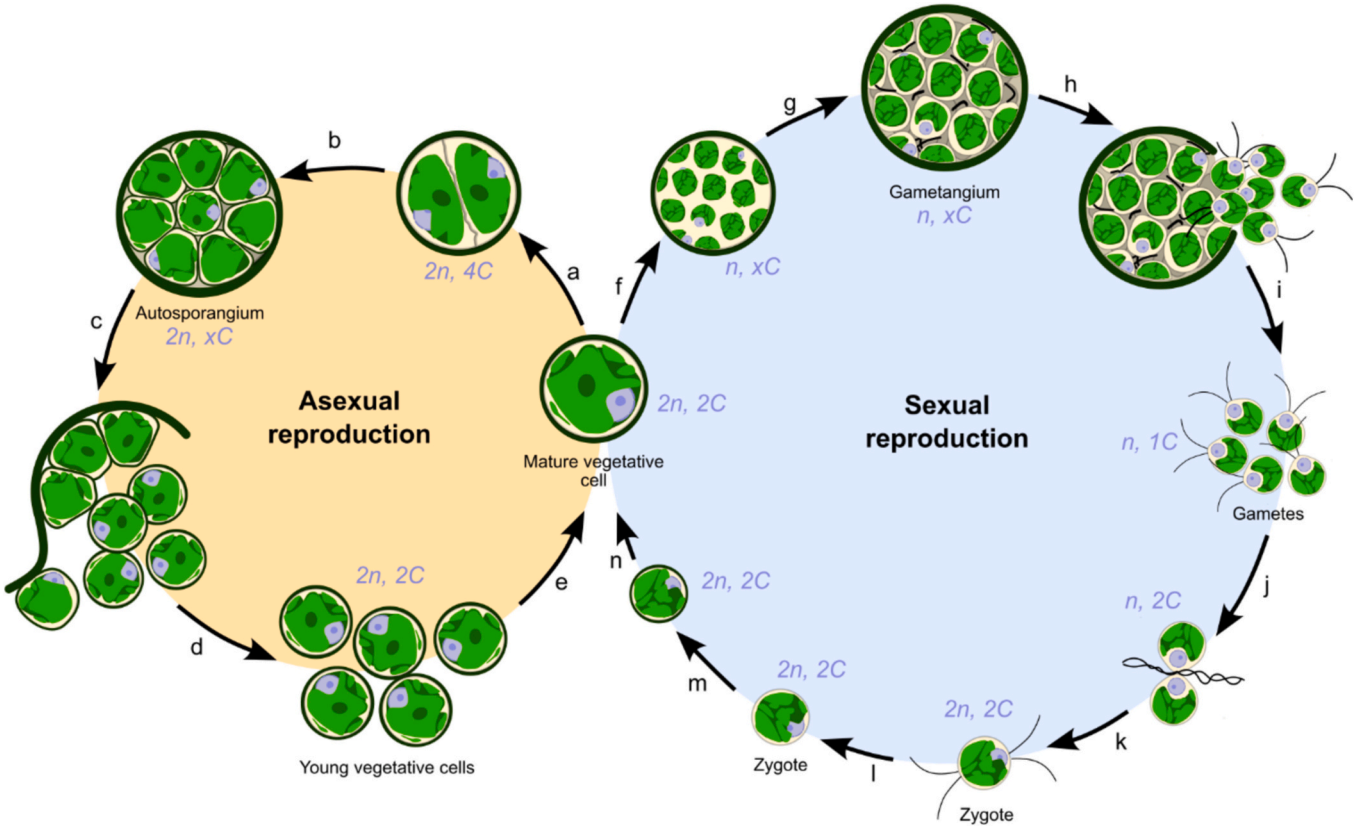

Fig. 5. The life cycle of *Trebouxia lynniae*. DNA content and nucleus ploidy level of the cells is indicated near each step: n = haploid, $2n$ = diploid, C is the total DNA charge. xC indicates stages in the life cycle for which the number of nuclei within the structure is unknown (*i.e.* gametangium) or variates within a range (between 4 and 32 for autosporangium). Each step of the life cycle is letter coded: *a*, chloroplast division and nuclear mitotic division; *b*, formation of symmetric autosporangium containing *2n* cell-walled cells; *c* and *d*, releasing of young vegetative cells out of the autosporangium; *e*, full development into mature vegetative cells; *f*, division of chloroplasts into globular structures and meiotic nuclear reduction; *g*, formation of gametangium with many cells without cell walls; *h* and *i*, releasing of motile gametes from the gametangium through an ostiolum; *j*, recognition and mating, contact and flagellar adhesion of gametes; *k*, plasmogamy, karyogamy and formation of *2n* tetra-flagellated zygotes; *l*, development of zygotes and loss of flagella; *m*, formation of cell wall; *n*, full development into mature vegetative cells.

4. Discussion

Our results confirm the hypothesis that *T. lynniae* has sexual reproduction and further describe it as having a diplontic life cycle and being isogamous. The allelic distribution obtained by nuclear sequencing would be that expected for a diploid organism which has undergone several generations of inbreeding (*i.e.*, retaining few heterozygous loci while the rest follow a process of fixation) such as the culturing conditions of the strain used for genotyping. In addition, *T. lynniae* genome contains the key genes involved in meiosis and mating, and it is able to express them. Although the presence of mating type-related genes, such as MID, MTD1 and FUS1, supports the existence of a mating system [77], we were not able of identifying the sex determining region using these genes. By analysing changes in DNA content during colony proliferation, together with changes in cell population frequencies, we were able to confirm zoospores to be gametes. The results obtained by microscopy DNA and cell wall staining further support this hypothesis.

Genome annotation comparison between Trebouxiophyceae genomes revealed the most robust annotation results for the *T. lynniae* assembly, that showed the highest percentages of genes with GO annotations and OrthoGroup assignments. The GO enrichment test for the genes exclusively found in *T. lynniae* highlights an overrepresentation of protein phosphorylation and magnesium transport processes, as well as membrane-located proteins (Fig. S5, Data S3). This suggests the existence of specific signalling and transport pathways in *T. lynniae*.

Although Streptophyta and Chlorophyta independently evolved on their path to earth, they experienced some similar events. On the one hand, both clades were associated with fungi during their terrestrialization, likely through mycorrhizal-like and lichen-like symbioses [1]. On the other hand, our results show an evolutionary convergence of the haploid-to-diploid transition. This implies that evolution from an aquatic haploid dominant to a terrestrial diploid dominant life cycle is common to both. While most aquatic species are described as haploid dominant in Chlorophyta [3], here we show a terrestrial species that is

diploid dominant, as it happens in Streptophyta. Moreover, another evolutionary convergence is the loss of some specific transcription factors that are related with the regulation of the life cycle. In plant haploid-dominant life cycles, the diploid phase is limited to a unicellular zygospore, the so-called "algal pattern" [78], governed by the TALE homeobox family of transcription factors universally present in Archaeplastida [74]. BELL-related TALE genes are present in genomes of green algae and absent from genomes of land plants, which instead carry true-BELL TALE genes. Hence, it was proposed that the loss of BELL-related genes participated in escaping from the haploid "algal pattern" throughout the case of the evolution of land plants [78]. A similar event may have occurred during the evolution of Trebouxiophyceae as we did not find any TALE homeobox transcription factors, supporting the proposed *T. lynniae* diplontic life cycle. It was also hypothesised that in a larger survey, other green organisms with diploid premeiotic spores would carry BELL-related genes and those with post-meiotic haploid spores would carry true-BELL genes [78]. However, our results, as well as the phylogeny of the TALE homeobox family, show that Trebouxiophyceae may be an exception to its universal presence in Archaeplastida [74]. Contrary to what happened in land plants, TALE genes have not been co-opted to new functions in Trebouxiophyceae.

Even though the use of the sugar-richer medium resulted in the production of a higher frequency of gametes than the poorer one, the described life cycle was basically the same. However, our findings show that the frequencies of each cell population differed between growth media and growth phases, which is in line with previous reports [35]. Asexual reproduction typically occurs during the exponential phase, while sexual reproduction tends to take place towards the end of the growth period when the algal population has reached a certain density [26], as observed in our experiments. These changes in cell population highlight the importance of accurately determining growth phases when interpreting physiological results and performing a taxonomical diagnosis.

In *Trebouxia,* high production of gametes was observed when growing in the glucose richer condition, which can be perceived as a decrease in the Redfield ratio (N:C). In most Volvocines gametogenesis is also triggered by nutrient perception, in particular nitrogen depletion. Volvocine is a diverse group that includes unicellular and colony-forming microalgae that can perform asexual and sexual reproduction. Despite having haplontic life cycle [79], multicellular Volvocines such as *Gonium* share some coincides with *Trebouxia* life cycle. While *Gonium* colonies multiply mainly by rounds of asexual cell fissions, *Trebouxia* colonies does so but by means of sporangia. Moreover, both *Gonium* and *Trebouxia* sexually reproduce under specific nutrient conditions through motile isogamous gametes that break apart from the colonies. This highlights a potential convergence in how these organisms disperse and potentially encounter compatible partners for sexual reproduction when environmental conditions become favourable.

Our findings challenge the notion that the presence of flagellated cells can be regarded as a taxonomic feature in *Trebouxia*. Instead, we emphasise that production of motile cells is contingent upon culture conditions and growth phase. Whether the triggering of sex is a response to population density itself [26] (*e.g.*, because it maximises the probability of gametes encounter) or it is used as a proxy for environmental signals [80] (*e.g.*, increase of nutrients or reduction of light), remains unclear. Within lichen thalli, *Trebouxia* species were reported to grow as stable consortia called "green modules" [81]. In such an environment, the cost of recombination and the loss of advantageous genetic combinations, the demographic cost of sex, could outweigh the benefits of diverse offspring [23,75,76]. How phycobionts growth is regulated and whether sexual reproduction occurs inside lichen thalli or not, is currently unknown. However, the existence of facultative sexual life cycles as we have shown for *T. lynniae* opens up an interesting window to the study of the costs of sex and its evolution and maintenance in a complex ecosystem such as a lichen thallus where inter and intraspecies conflicts can occur. Fungal symbionts would benefit from controlling sexual reproduction of the phycobiont (for example through nutrient control), either to prevent it, avoiding the formation of less suitable photobiont genotypes (the recombinational cost of sex) [23] or to promote it to provide a genetically diverse collection of photobionts when the fungus is asexually reproducing through diaspores. A pool of genetically diverse algae could help to cope with novel environments. For the algae, combining sexual and asexual reproduction with density-dependent induction can also be an advantageous strategy [82]. Within the thallus, rapid asexual growth would help to outgrow competing species, or less fitted genotypes [83], without incurring in the demographic or recombinational cost of sex. However, switching to sexual reproduction when populations densities are high could be beneficial, on the one hand, by increasing the probability of gamete encounters, and on the other, investing in sex when competition is higher reduces the recombination cost (*i.e.*, the risk of being excluded by competition compensates for the cost of producing less fitted offspring). Additionally, high phycobionts population densities could be interpreted as a cue to leave the thallus. In such a case, the production of a genetically variable offspring in a complex environment as the lichen holobiome would be advantageous to initiate new symbiotic interactions to cope with a new environment. In this way, the microalga cyclically integrates in a new unit forming a new thallus, *i.e.*, cyclic symbiosis [84,85].

Our findings regarding sexual reproduction of *T. lynniae* have important implications when considering the high diversity observed within the *Trebouxia* genus [9,86]. This reproductive strategy may contribute to the generation and maintenance of genetic diversity. This is particularly relevant considering the evolution and ecological adaptation of *Trebouxia* species [10,87] to diverse and extreme environments in which they are reported as lichen symbionts [9]. The ability to undergo sexual reproduction may confer an advantage under stressful environmental conditions by promoting exchange and recombination of genetic material as reported in other organisms [88,89]. Lichen reproduce by propagules and/or by *de novo* formation, both are frequent processes depending on the lichen species. The later, suggests that the germinating mycobiont spore has to find a phycobiont in non-symbiotic state. Whether these algae are able to reproduce sexually within the lichen or between cycles of lichenized and free living states (cyclic symbiosis), remains unclear. Recently, Veselá et al. [16] have reviewed the lifestyle of lichen chlorobionts, indicating that *Trebouxia* genus is one of the most common genera of free-living microalgae in nature. As Veselá et al. [16], this manuscript also aim to shed some light into the complex nature of phycobiont life cycles and lichen symbioses. The discovery of sexual reproduction in *T. lynniae* thus expands our understanding of the ecological and evolutionary dynamics within *Trebouxia* and highlights the potential adaptive significance of sex in the face of challenging and changing ecological conditions.

Supplementary data to this article can be found online at https://doi.org/10.1016/j.algal.2024.103744.

CRediT authorship contribution statement

Ayelén Gazquez: Writing – review & editing, Writing – original draft, Visualization, Validation, Software, Methodology, Investigation, Formal analysis, Conceptualization. **César Daniel Bordenave:** Writing – review & editing, Writing – original draft, Visualization, Validation, Software, Methodology, Investigation, Formal analysis, Conceptualization. **Javier Montero-Pau:** Writing – review & editing, Writing – original draft, Visualization, Validation, Software, Methodology, Investigation, Formal analysis, Data curation, Conceptualization. **Marta Pérez-Rodrigo:** Writing – review & editing, Investigation, Formal analysis. **Francisco Marco:** Writing – review & editing, Investigation, Formal analysis. **Fernando Martínez-Alberola:** Writing – review & editing, Investigation, Formal analysis. **Lucia Muggia:** Writing – review & editing, Writing – original draft, Supervision, Conceptualization. **Eva Barreno:** Writing – review & editing, Supervision, Resources, Project administration, Funding acquisition, Conceptualization. **Pedro**

Carrasco: Writing – review & editing, Supervision, Resources, Project administration, Funding acquisition, Conceptualization.

Declaration of competing interest

The authors declare that they have no known competing financial interests or personal relationships that could have appeared to influence the work reported in this paper.

Acknowledgements

We thank the members of the SYMBIOGENE research group for discussions. Funding for this study was provided by PROMETEO Excellence in Research Program (PROMETEO/2021/005, Generalitat Valenciana, Spain), to EB and PC, and Grant PID2021-127087NB-100 funded by MCIN/AEI/10.13039/501100011033, to PC. CDB, received funding from a postdoctoral contract María Zambrano of Ministerio de Universidades, Next Generation UE (grant ZA21-046). AG received funding from a postdoctoral contract of Generalitat Valenciana and European Social Fund (APOSTD21). MP-R received funding from a PhD contract of European Space agency (IDEA: I-2021-05232) and PROMETEO Excellence in Research Program (PROMETEO/2021/005, Generalitat Valenciana, Spain). Flow cytometry and microscopy experiments were performed in the cell cultures and cytometry and the microscopy sections, respectively, of the SCSIE (Central Service for Experimental Research) of the Universitat de València Burjassot-Paterna Campus.

Data availability

The raw genomic and transcriptomic sequence data reported in this paper have been deposited in NCBI SRA under BioProject PRJNA996335 and the whole genome assembly under accession number JAVLRR000000000. Genome structural and functional annotations have been deposited in Zenodo and available at DOI: https://zenodo.org/records/10074968. All other data are available in the article and its Supplementary files or from the corresponding authors upon request.

References

[1] F. Lutzoni, M.D. Nowak, M.E. Alfaro, V. Reeb, J. Miadlikowska, M. Krug, A. E. Arnold, L.A. Lewis, D.L. Swofford, D. Hibbett, et al., Contemporaneous radiations of fungi and plants linked to symbiosis, Nat. Commun. 9 (2018) 5451.
[2] R.M. McCourt, L.A. Lewis, P.K. Strother, C.F. Delwiche, N.J. Wickett, J. De Vries, J. L. Bowman, Green land: multiple perspectives on green algal evolution and the earliest land plants, Am. J. Bot. 110 (2023) e16175.
[3] K.J. Niklas, U. Kutschera, The evolution of the land plant life cycle, New Phytol. 185 (2010) 27–41.
[4] V. Ahmadjian, Some new and interesting species of *Trebouxia*, a genus of lichenized algae, Am. J. Bot. 47 (1960) 677–683.
[5] P.A. Archibald, *Trebouxia* de Pulmaly (Chlorophyceae, Chlorococcales) and *Pseudotrebouxia* gen. nov. (Chlorophyceae, Chlorosarcinales)*, Phycologia 14 (1975) 125–137.
[6] T. Friedl, Comparative ultrastructure of pyrenoids in *Trebouxia* (Microthamniales, Chlorophyta), Plant Syst. Evol. 164 (1989) 145–159.
[7] T. Friedl, New aspects of the reproduction by autospores in the lichen alga *Trebouxia* (Microthamniales, Chlorophyta), Archiv für Protistenkunde : Protozoen, Algen, Pilze 143 (1993) 153–161.
[8] E. Tschermak-Woess, Developmental studies in trebouxioid algae and taxonomical consequences, Plant Systematics and Evolution 164 (1989) 161–195.
[9] R. De Carolis, A. Cometto, P. Moya, E. Barreno, M. Grube, M. Tretiach, S.D. Leavitt, L. Muggia, Photobiont diversity in lichen symbioses from extreme environments, Front. Microbiol. 13 (2022).
[10] M.P. Nelsen, S.D. Leavitt, K. Heller, L. Muggia, H.T. Lumbsch, Macroecological diversification and convergence in a clade of keystone symbionts, FEMS Microbiol. Ecol. 97 (2021) 72.
[11] T. Spribille, P. Resl, D.E. Stanton, G. Tagirdzhanova, Evolutionary biology of lichen symbioses, New Phytol. 234 (2022) 1566–1582.
[12] L. Muggia, S. Leavitt, E. Barreno, The hidden diversity of lichenised Trebouxiophyceae (Chlorophyta), Phycologia 57 (2018) 503–524.
[13] P. Škaloud, J. Steinová, T. Řídká, L. Vančurová, O. Peksa, Assembling the challenging puzzle of algal biodiversity: species delimitation within the genus *Asterochloris* (Trebouxiophyceae, Chlorophyta), J. Phycol. 51 (2015) 507–527.
[14] C.D. Bordenave, L. Muggia, S. Chiva, S.D. Leavitt, P. Carrasco, E. Barreno, Chloroplast morphology and pyrenoid ultrastructural analyses reappraise the diversity of the lichen phycobiont genus *Trebouxia* (Chlorophyta), Algal Res. 61 (2022) 102561.
[15] P. Škaloud, O. Peksa, Comparative study of chloroplast morphology and ontogeny in *Asterochloris* (Trebouxiophyceae, Chlorophyta), Biologia (2008) 873–880.
[16] V. Veselá, V. Malavasi, P. Škaloud, A synopsis of green-algal lichen symbionts with an emphasis on their free-living lifestyle, Phycologia (2024) 1–22.
[17] M. Melkonian, E. Peveling, Zoospore ultrastructure in species of *Trebouxia* and *Pseudotrebouxia* (Chlorophyta)*, Plant Systematics and Evolution 158 (1988) 183–210.
[18] P.G. Hofstatter, G.M. Ribeiro, A.L. Porfírio-Sousa, D.J.G. Lahr, The sexual ancestor of all eukaryotes: a defense of the "meiosis toolkit", BioEssays 42 (2020) 2000037.
[19] S.-B. Malik, A.W. Pightling, L.M. Stefaniak, A.M. Schurko, J.M. Logsdon, An expanded inventory of conserved meiotic genes provides evidence for sex in *Trichomonas vaginalis*, PloS One 3 (2008) 2879.
[20] A.M. Schurko, J.M. Logsdon, Using a meiosis detection toolkit to investigate ancient asexual "scandals" and the evolution of sex, BioEssays 30 (2008) 579–589.
[21] D. Armaleo, O. Müller, F. Lutzoni, Ó.S. Andrésson, G. Blanc, H.B. Bode, F. R. Collart, F. Dal Grande, F. Dietrich, I.V. Grigoriev, et al., The lichen symbiosis re-viewed through the genomes of *Cladonia grayi* and its algal partner *Asterochloris glomerata*, BMC Genomics 20 (2019) 1–33.
[22] K. Fučíková, M. Pažoutová, F. Rindi, Meiotic genes and sexual reproduction in the green algal class Trebouxiophyceae (Chlorophyta), J. Phycol. 51 (2015) 419–430.
[23] S. Kroken, J.W. Taylor, Phylogenetic species, reproductive mode, and specificity of the green alga *Trebouxia* forming lichens with the fungal genus *Letharia*, Bryologist 103 (2000) 645–660.
[24] M. Arora, D. Sahoo, Growth forms and life histories in green algae, in: D. Sahoo, J. Seckbach (Eds.), Cellular Origin, Life in Extreme Habitats and Astrobiology, The Algae World, Springer Netherlands, Dordrecht, 2015, pp. 121–175.
[25] S.-N. Bai, The concept of the sexual reproduction cycle and its evolutionary significance, Frontiers in Plant Science 6 (2015).
[26] S.C. Agrawal, Factors controlling induction of reproduction in algae—review: the text, Folia Microbiologica 57 (2012) 387–407, 2012. 5 57.
[27] J. Van Etten, L.F. Benites, T.G. Stephens, H.S. Yoon, D. Bhattacharya, Algae obscura: the potential of rare species as model systems, Journal of Phycology 59 (2023) 293–300.
[28] E. Barreno, L. Muggia, S. Chiva, A. Molins, C. Bordenave, F. García-Breijo, P. Moya, *Trebouxia lynnae* sp. nov. (former *Trebouxia* sp. TR9): biology and biogeography of an epitome lichen symbiotic microalga, Biology 11 (2022) 1196.
[29] C.D. Bordenave, F. García-Breijo, A. Gazquez, L. Muggia, P. Carrasco, E. Barreno, Low Temperature Scanning Electron Microscopy (LTSEM) Findings on the Ultrastructure of *Trebouxia lynnae* (Trebouxiophyceae, Lichenized Microalgae), 2023.
[30] R. Álvarez, A. del Hoyo, C. Díaz-Rodríguez, A.J. Coello, E.M. del Campo, E. Barreno, M. Catalá, L.M. Casano, Lichen rehydration in heavy metal-polluted environments: Pb modulates the oxidative response of both *Ramalina farinacea* thalli and its isolated microalgae, Microb. Ecol. 69 (2015) 698–709.
[31] R. Álvarez, A. del Hoyo, F. García-Breijo, J. Reig-Armiñana, E.M. del Campo, A. Guéra, E. Barreno, L.M. Casano, Different strategies to achieve Pb-tolerance by the two *Trebouxia* algae coexisting in the lichen *Ramalina farinacea*, J. Plant Physiol. 169 (2012) 1797–1806.
[32] L.M. Casano, M.R. Braga, R. Álvarez, E.M. del Campo, E. Barreno, Differences in the cell walls and extracellular polymers of the two *Trebouxia* microalgae coexisting in the lichen *Ramalina farinacea* are consistent with their distinct capacity to immobilize extracellular Pb, Plant Sci. 236 (2015) 195–204.
[33] L.M. Casano, E.M. Del Campo, F.J. García-Breijo, J. Reig-Armiñana, F. Gasulla, A. Del Hoyo, A. Guéra, E. Barreno, Two *Trebouxia* algae with different physiological performances are ever-present in lichen thalli of *Ramalina farinacea*. Coexistence versus competition? Environ. Microbiol. 13 (2011) 806–818.
[34] D.C. Centeno, A.F. Hell, M.R. Braga, E.M. del Campo, L.M. Casano, Contrasting strategies used by lichen microalgae to cope with desiccation–rehydration stress revealed by metabolite profiling and cell wall analysis, Environ. Microbiol. 18 (2016) 1546–1560.
[35] N. Domínguez-Morueco, H. Moreno, E. Barreno, M. Catalá, Preliminary assessment of terrestrial microalgae isolated from lichens as testing species for environmental monitoring: lichen phycobionts present high sensitivity to environmental micropollutants, Ecotoxicol. Environ. Saf. 99 (2014) 35–44.
[36] J.R. Expósito, I. Mejuto, M. Catalá, Detection of active cell death markers in rehydrated lichen thalli and the involvement of nitrogen monoxide (NO), Symbiosis 82 (2020) 59–67.
[37] M. González-Hourcade, E.M. del Campo, L.M. Casano, The under-explored extracellular proteome of aero-terrestrial microalgae provides clues on different mechanisms of desiccation tolerance in non-model organisms, Microb. Ecol. 81 (2021) 437–453.
[38] A.F. Hell, F. Gasulla, M. González-Houcarde, M.T. Pelegrino, A.B. Seabra, E.M. del Campo, L.M. Casano, D.C. Centeno, Polyols-related gene expression is affected by cyclic desiccation in lichen microalgae, Environ. Exp. Bot. 185 (2021) 104397.
[39] E. Hinojosa-Vidal, F. Marco, F. Martínez-Alberola, F.J. Escaray, F.J. García-Breijo, J. Reig-Armiñana, P. Carrasco, E. Barreno, Characterization of the responses to saline stress in the symbiotic green microalga *Trebouxia* sp. TR9, Planta 248 (2018) 1473–1486.
[40] A. del Hoyo, R. Álvarez, E.M. del Campo, F. Gasulla, E. Barreno, L.M. Casano, Oxidative stress induces distinct physiological responses in the two *Trebouxia* phycobionts of the lichen Ramalina farinacea, Ann. Bot. 107 (2011) 109–118.

[41] H. Moreno Traba, N. Domínguez-Morueco, E. Barreno, M. Catalá, Lichen microalgae are sensitive to environmental concentrations of atrazine, J. Environ. Sci. Health B 52 (2017) 223–228.
[42] F. Martínez-Alberola, E. Barreno, L.M. Casano, F. Gasulla, A. Molins, E.M. del Campo, Dynamic evolution of mitochondrial genomes in Trebouxiophyceae, including the first completely assembled mtDNA from a lichen-symbiont microalga (*Trebouxia* sp. TR9), Scientific Reports 9 (2019) 1–12, 2019 9:1.
[43] F. Martínez-Alberola, E. Barreno, L.M. Casano, F. Gasulla, A. Molins, P. Moya, M. González-Hourcade, E.M. del Campo, The chloroplast genome of the lichen-symbiont microalga *Trebouxia* sp. Tr9 (Trebouxiophyceae, Chlorophyta) shows short inverted repeats with a single gene and loss of the rps4 gene, which is encoded by the nucleus, J. Phycol. 56 (2020) 170–184.
[44] H. Bischoff, H. Bold, Some soil algae from enchanted rock and related algal species, Phycological Studies IV (1963) 1–95.
[45] F. Gasulla, A. Guéra, E. Barreno, A simple and rapid method for isolating lichen photobionts, Symbiosis 51 (2010) 175–179.
[46] D.R. Zerbino, E. Birney, Velvet: algorithms for de novo short read assembly using de Bruijn graphs, Genome Res. 18 (2008) 821–829.
[47] A. Gurevich, V. Saveliev, N. Vyahhi, G. Tesler, QUAST: quality assessment tool for genome assemblies, Bioinformatics 29 (2013) 1072–1075.
[48] M. Manni, M.R. Berkeley, M. Seppey, F.A. Simão, E.M. Zdobnov, BUSCO update: novel and streamlined workflows along with broader and deeper phylogenetic coverage for scoring of eukaryotic, prokaryotic, and viral genomes (J Kelley, Ed.), Mol. Biol. Evol. 38 (2021) 4647–4654.
[49] C.L. Weiß, M. Pais, L.M. Cano, S. Kamoun, H.A. Burbano, nQuire: a statistical framework for ploidy estimation using next generation sequencing, BMC Bioinformatics 19 (2018) 122.
[50] I. Korf, Gene finding in novel genomes, BMC Bioinformatics 5 (2004) 59.
[51] M. Stanke, M. Diekhans, R. Baertsch, D. Haussler, Using native and syntenically mapped cDNA alignments to improve de novo gene finding, Bioinformatics 24 (2008) 637–644.
[52] P.J. Ferris, E.V. Armbrust, U.W. Goodenough, Genetic structure of the mating-type locus of *Chlamydomonas reinhardtii*, Genetics 160 (2002) 181–200.
[53] P.J. Ferris, U.W. Goodenough, Mating type in Chlamydomonas is specified by mid, the minus-dominance gene, Genetics 146 (1997) 859.
[54] P.J. Ferris, J.P. Woessner, U.W. Goodenough, A sex recognition glycoprotein is encoded by the plus mating-type gene fus1 of *Chlamydomonas reinhardtii*, Mol. Biol. Cell 7 (1996) 1235–1248.
[55] P.G. Hofstatter, M.W. Brown, D.J.G. Lahr, Comparative genomics supports sex and meiosis in diverse Amoebozoa, Genome Biol. Evol. 10 (2018) 3118–3128.
[56] P.G. Hofstatter, D.J.G. Lahr, All eukaryotes are sexual, unless proven otherwise, BioEssays 41 (2019) 1800246.
[57] S.S. Merchant, S.E. Prochnik, O. Vallon, E.H. Harris, S.J. Karpowicz, G.B. Witman, A. Terry, A. Salamov, L.K. Fritz-Laylin, L. Maréchal-Drouard, et al., The *Chlamydomonas* genome reveals the evolution of key animal and plant functions, Science 318 (2007) 245–250.
[58] M.J. Misamore, S. Gupta, W.J. Snell, The *Chlamydomonas* Fus1 protein is present on the mating type plus fusion organelle and required for a critical membrane adhesion event during fusion with minus gametes, Mol. Biol. Cell 14 (2003) 2530–2542.
[59] J. Ning, T.D. Otto, C. Pfander, F. Schwach, M. Brochet, E. Bushell, D. Goulding, M. Sanders, P.A. Lefebvre, J. Pei, et al., Comparative genomics in *Chlamydomonas* and *Plasmodium* identifies an ancient nuclear envelope protein family essential for sexual reproduction in protists, fungi, plants, and vertebrates, Genes Dev. 27 (2013) 1198–1215.
[60] J. Schindelin, I. Arganda-Carreras, E. Frise, V. Kaynig, M. Longair, T. Pietzsch, S. Preibisch, C. Rueden, S. Saalfeld, B. Schmid, et al., Fiji: an open-source platform for biological-image analysis, Nature Methods 9 (2012) 676–682, 2012 9:7.
[61] R Core Team, R: A Language and Environment for Statistical Computing. https://www.R-project.org/, 2021.
[62] RStudio Team, RStudio: Integrated Development Environment for R. http://www.rstudio.com/, 2021.
[63] H. Wickham, stringr: Simple, Consistent Wrappers for Common String Operations. https://stringr.tidyverse.org, 2022. https://github.com/tidyverse/stringr.
[64] H. Wickham, R. François, L. Henry, K. Müller, D. Vaughan, dplyr: A Grammar of Data Manipulation. https://dplyr.tidyverse.org, 2023. https://github.com/tidyverse/dplyr.
[65] H. Wickham, J. Hester, J. Bryan, readr: Read Rectangular Text Data. https://readr.tidyverse.org, 2023. https://github.com/tidyverse/readr.
[66] H. Wickham, D. Vaughan, M. Girlich, tidyr: Tidy Messy Data. https://tidyr.tidyverse.org, 2023. https://github.com/tidyverse/tidyr.
[67] T.V. Elzhov, K.M. Mullen, A.N. Spiess, B. Bolker, minpack. lm: R interface to the Levenberg-Marquardt nonlinear least-squares algorithm found in MINPACK, plus support for bounds. https://cran.r-project.org/web/packages/minpack.lm/index.html, 2016.
[68] H. Wickham, ggplot2: Elegant Graphics for Data Analysis, Springer, Switzerland, 2016.
[69] I. Ulrich, W. Ulrich, Flow Cytometric DNA-Analysis of Plant Protoplasts Stained With DAPI, 1986.
[70] D. Čertnerová, Nuclei isolation protocols for flow cytometry allowing nuclear DNA content estimation in problematic microalgal groups, J. Appl. Phycol. 33 (2021) 2057–2067.
[71] D. Hammill, CytoExploR: Interactive Analysis of Cytometry Data, 2021. R package version 1.1.0.
[72] H.M. Shapiro, N.G. Perlmutter, Violet laser diodes as light sources for cytometry, Cytometry: The Journal of the International Society for Analytical Cytology 44 (2) (2001) 133–136.
[73] B. Münch, P. Trtik, F. Marone, M. Stampanoni, Stripe and ring artifact removal with combined wavelet — Fourier filtering, Optics Express 17 (10) (2009) 8567–8591, 17: 8567–8591.
[74] S. Joo, M.H. Wang, G. Lui, J. Lee, A. Barnas, E. Kim, S. Sudek, A.Z. Worden, J.-H. Lee, Common ancestry of heterodimerizing TALE homeobox transcription factors across Metazoa and Archaeplastida, BMC Biol. 16 (2018) 136.
[75] J. Maynard Smith, The Evolution of Sex, Cambridge University Press, Cambridge [Eng.]; New York, 1978.
[76] U. Goodenough, J.-H. Lee, W.J. Snell, The sexual cycle, in: The *Chlamydomonas* Sourcebook, Elsevier, 2023, pp. 211–254.
[77] K. Yamamoto, T. Hamaji, H. Kawai-Toyooka, R. Matsuzaki, F. Takahashi, Y. Nishimura, M. Kawachi, H. Noguchi, Y. Minakuchi, J.G. Umen, et al., Three genomes in the algal genus *Volvox* reveal the fate of a haploid sex-determining region after a transition to homothallism, Proc. Natl. Acad. Sci. U. S. A. 118 (2021) e2100712118.
[78] J.-H. Lee, H. Lin, S. Joo, U. Goodenough, Early sexual origins of homeoprotein heterodimerization and evolution of the plant KNOX/BELL family, Cell 133 (2008) 829–840.
[79] J.G. Umen, *Volvox* and volvocine green algae, EvoDevo 11 (1) (2020) 13.
[80] A.F. Mohsen, A.F. Khaleata, M.A. Hashem, A. Metwalli, Effect of different nitrogen sources on growth, reproduction, amino acid, fat and sugar contents in *Ulva fasciata* Delile (part III), Bot. Mar. 17 (1974).
[81] U. Goodenough, R. Wagner, R. Roth, Lichen 4. The Algal Layer, in: Algal Research, 58, 2021, p. 102355.
[82] King Serra, Optimal rates of bisexual reproduction in cyclical parthenogens with density-dependent growth, J. Evol. Biol. 12 (1999) 263–271.
[83] A. Molins, P. Moya, L. Muggia, E. Barreno, Thallus growth stage and geographic origin shape microalgal diversity in *Ramalina farinacea* Lichen holobionts, J. Phycol. 57 (2021) 975–987.
[84] M.J. Chapman, L. Margulis, Morphogenesis by Symbiogenesis 1, 1998, pp. 319–326.
[85] R. Guerrero, L. Margulis, M. Berlanga, Symbiogenesis: the holobiont as a unit of evolution, Int. Microbiol. (2013) 133–143.
[86] L. Muggia, M.P. Nelsen, P.M. Kirika, E. Barreno, A. Beck, H. Lindgren, H. T. Lumbsch, S.D. Leavitt, Formally described species woefully underrepresent phylogenetic diversity in the common lichen photobiont genus *Trebouxia* (Trebouxiophyceae, Chlorophyta): an impetus for developing an integrated taxonomy, Mol. Phylogenet. Evol. 149 (2020).
[87] M.P. Nelsen, R. Lücking, C.K. Boyce, H.T. Lumbsch, R.H. Ree, The macroevolutionary dynamics of symbiotic and phenotypic diversification in lichens, Proc. Natl. Acad. Sci. U. S. A. 117 (2020) 21495–21503.
[88] J.C. Gray, M.R. Goddard, Sex enhances adaptation by unlinking beneficial from detrimental mutations in experimental yeast populations, BMC Evol. Biol. 12 (2012) 1–11.
[89] P. Luijckx, E.K. Ho Ho, M. Gasim, S. Chen, A. Stanic, C. Yanchus, Y.S. Kim, A. F. Agrawal, Higher rates of sex evolve during adaptation to more complex environments, Proc. Natl. Acad. Sci. U. S. A. 114 (2017) 534–539.